Biophysical Journal, Volume *116*

Supplemental Information

Membrane-Binding Cooperativity and Coinsertion by C2AB Tandem Domains of Synaptotagmins 1 and 7

Hai T. Tran, Lauren H. Anderson, and Jefferson D. Knight

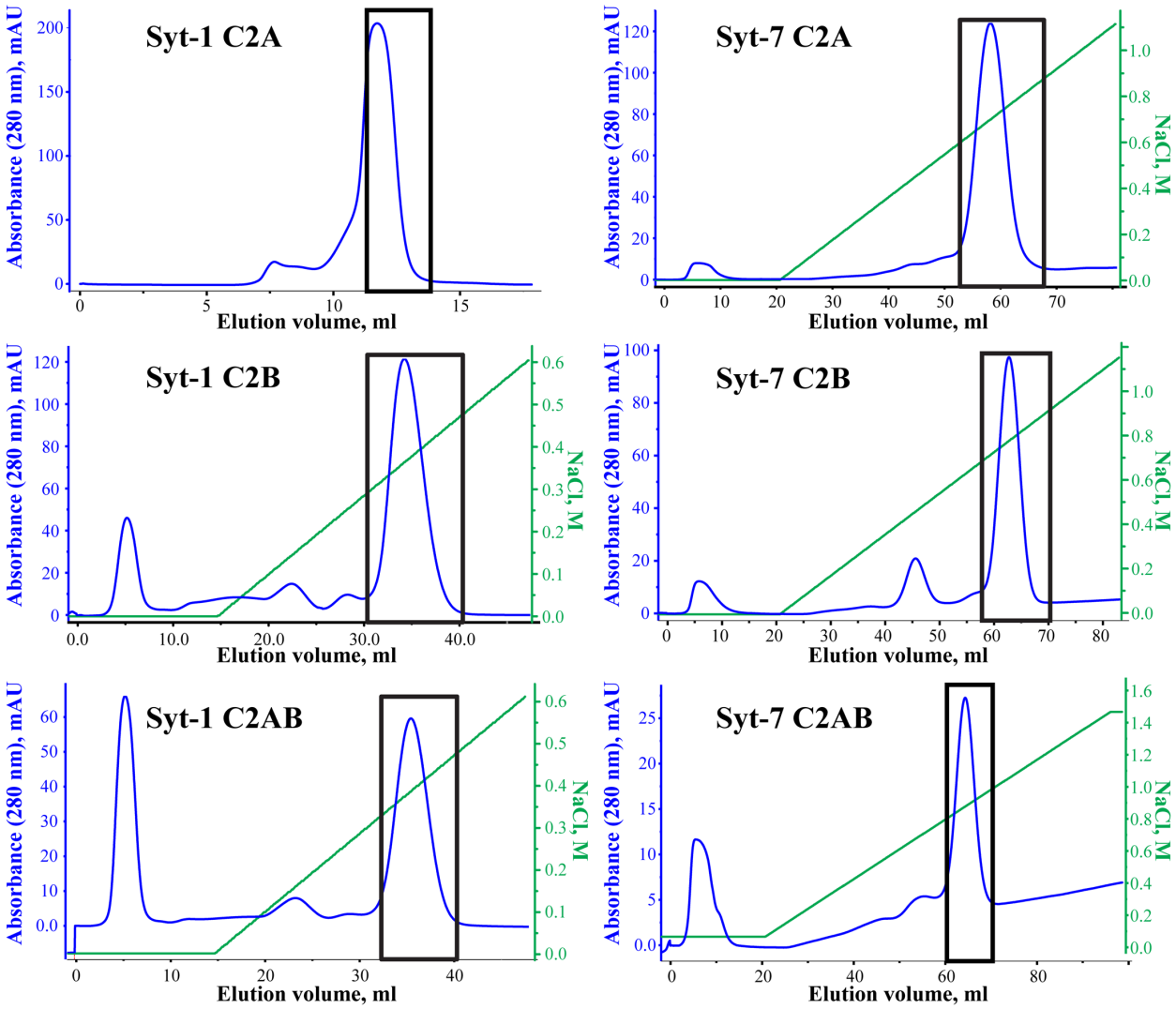

Figure S1. Gel filtration (Syt-1 C2A) and cation exchange (other C2 domains) chromatograms. Syt-1 C2A has a negative net charge and was purified by gel filtration chromatography using an isocratic elution to remove any aggregates. All other C2 fragments were purified by cation exchange chromatography to remove anionic contaminants. All were performed in Buffer A (with 1 mM βME for ion exchange runs) and ion exchange runs were eluted with added NaCl as indicated in green. Absorbance chromatograms at 280 nm are shown in blue. A peak prior to NaCl indicated presence of anionic contaminants; these flow-through peaks typically had absorbance spectra consistent with nucleic acid. Fractions corresponding to the boxed regions were combined and buffer-exchanged to remove excess NaCl. Baseline drift, as seen in Syt-7 C2AB chromatogram is likely due to a nonzero level of disulfide-linked βME in the high-salt elution buffer.

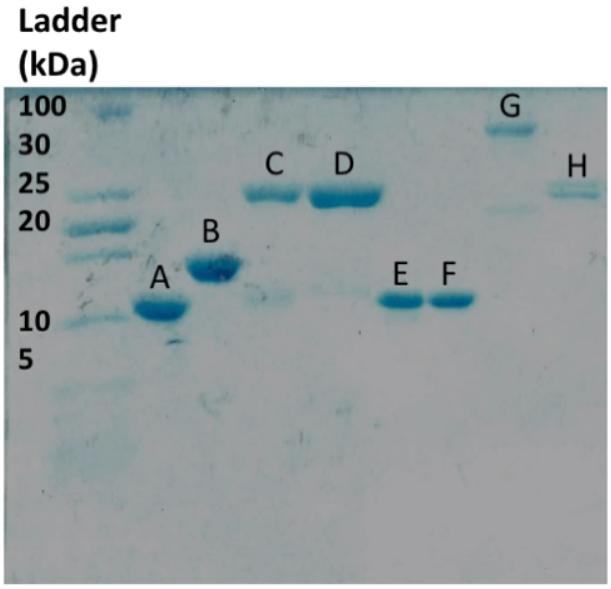

Figure S2. SDS-PAGE analysis of protein samples after gel filtration or cation exchange. **A**: Syt-1 C2A; **B**: Syt-1 C2B; **C, D**: Syt-1 C2AB from two different aliquots of protein; **E:** Syt-7 C2A; **F**: Syt-7 C2B; **G:** GST-tagged fusion protein of Syt-7 C2AB; **H**: Syt-7 C2AB, final purified protein used for this study. All protein samples have the expected mass.

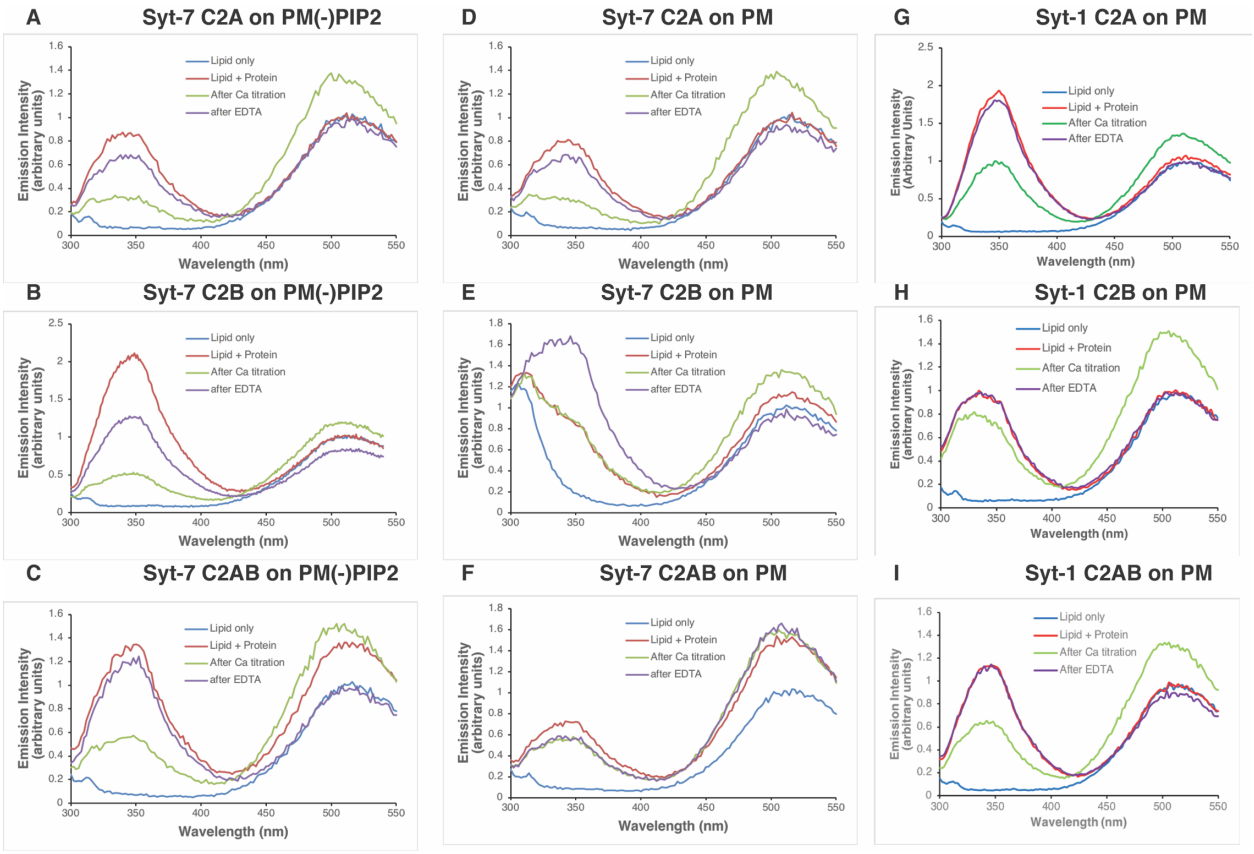

Figure S3: Fluorescence emission scans before and after Ca^{2+} titrations. Emission spectra were measured of the indicated liposomes in the absence of protein (blue), in an identical sample containing the indicated Syt-7 or Syt-1 C2 domain prior to Ca^{2+} addition (red), after the addition of Ca^{2+} to the highest concentration used (see Figure 2) (green), and after addition of 2 mM EDTA (violet). Peaks at 350 nm correspond to tryptophan (donor) emission, and peaks at 510 nm correspond to dansyl (acceptor) emission. Protein-membrane binding is assessed and quantified from increased acceptor emission. The large scatter peak at lower wavelengths in panel E is due to instrument settings (wider emission slit) and does not affect quantitation of acceptor emission. Spectra after titration are corrected for dilution and normalized to dansyl emission in the lipid-only samples. We note that some of the dansyl emission peaks "after EDTA" are slightly lower than before the titration. The effect, when present, is modest and should not affect interpretation of the titration data. We speculate it could arise due to small sample losses during titration (e.g., liposomes sticking to pipette tips used for Ca^{2+} additions, which could become stickier with certain proteins bound).

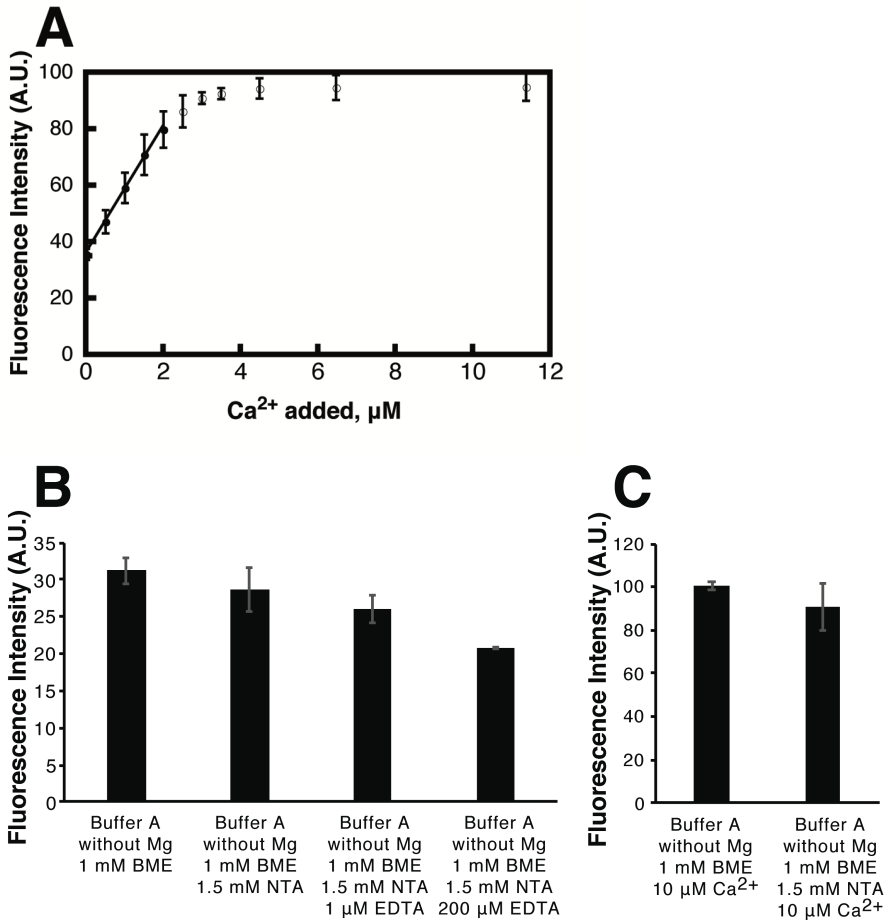

Figure S4: Measurement of background Ca^{2+} levels using the fluorescent Ca^{2+} chelator Quin-2. **A:** A solution of ~6 µM Quin-2 (Sigma-Aldrich) was prepared in Buffer A without Mg^{2+} and mixed 1:1 with the same buffer. This solution was titrated with Ca^{2+} prepared from a standard solution of known concentration (Ricca Chemical). Quin-2 fluorescence (ex. 345 nm, em. 505 nm) increased linearly upon addition of Ca^{2+} up to 2 µM (filled circles, best-fit line) with a slope of 22.5 arbitrary fluorescence units (A.U.)/µM, and became saturated at higher Ca^{2+} concentrations (open circles). Note that the Quin-2 concentration is not known precisely, and the y-intercept does not necessarily reflect zero Ca^{2+} because the solution may contain some background level of Ca^{2+}. **B:** In order to measure background Ca^{2+} levels in the "Ca^{2+}-free" buffers used for equilibrium Ca^{2+} titrations in Figures 2 and S5, these buffers were mixed 1:1 with the ~6-µM Quin-2 solution described above, and their fluorescence intensities were measured for direct comparison to the standard curve shown in A. (Mg^{2+} was omitted, as it also binds Quin-2 at the concentrations used in this study.) All of the measured intensities were below that of the y-intercept in the standard curve, indicating that these solutions have less background Ca^{2+} than the solution used for the standard curve. Inclusion of NTA had little effect on Quin-2 fluorescence, as NTA (K_d 115 µM) is a weak Ca^{2+} chelator compared to Quin-2 (K_d 115 nM) (1). However, addition of EDTA (K_d 24.3 nM) decreased Quin-2 fluorescence by up to ~30%, indicating the presence of some background Ca^{2+} in this buffer. **C:** Addition of 10 µM Ca^{2+} to solutions used in panel **B** brought the fluorescence intensity up to the saturation value measured in panel **A**. All error bars represent standard deviations from measurements performed in triplicate.

For calculating the amount of background Ca^{2+}, we assume that the level of Quin-2 fluorescence measured in the presence of 200 μM EDTA corresponds to zero Quin-2 bound to Ca^{2+}, (i.e. the "true" y-intercept of the standard curve). This assumption makes sense because (a) the excess EDTA is calculated to bind >99% of the Ca^{2+} away from Quin-2 based on the K_d values listed above, and (b) Quin-2 fluorescence is reported to increase 5-fold upon saturation with Ca^{2+} (1) consistent with its increase from ~20 to ~100 A.U. in this assay. Thus, using the 200 μM EDTA baseline value (Panel B, right) and the slope from Panel A, we calculate the background Ca^{2+} level in Buffer A without Mg^{2+} plus 1 mM BME (Panel B, left) to be 0.5 μM. NTA does not contribute a significant amount of background Ca^{2+} (Panel B, second from left). Other possible sources of Ca^{2+} contamination in our experiments in Figure 2 are considered below:

1. Protein stocks are unlikely to contribute significantly because these were dialyzed into Ca^{2+}-free buffer prior to use.
2. Liposome stocks are unlikely to contribute significantly because these were incubated with Chelex beads prior to use.
3. The $MgCl_2$ stock used lists a maximum Ca^{2+} content of 0.01% per ACS specifications, so the use of 1.2 mM $MgCl_2$ in our titration buffer solutions may contribute up to ~0.1 μM additional Ca^{2+}, bringing the total background Ca^{2+} concentration to ~0.6 μM.

Finally, we note that our use of Ca^{2+}-buffering systems decreases the level of free Ca^{2+} far below the total background level measured here. In our Ca^{2+} buffering system containing 1.5 mM NTA, the presence of 0.6 μM total Ca^{2+} would only include 40 nM free Ca^{2+}. Similarly, in our Ca^{2+} buffering system containing 1.5 mM NTA and 200 μM EDTA, the presence of 0.6 μM total Ca^{2+} would only include 75 pM free Ca^{2+}. MaxChelator (https://somapp.ucdmc.ucdavis.edu/pharmacology/bers/maxchelator/webmaxc/webmaxcE.htm) was used for all calculations of free Ca^{2+}. Thus, we can be confident that protein-to-membrane FRET measured in these systems prior to Ca^{2+} addition reflects a Ca^{2+}-independent protein-lipid interaction.

1. Tsien, R. Y., T. Pozzan, and T. J. Rink. 1982. Calcium homeostasis in intact lymphocytes: cytoplasmic free calcium monitored with a new, intracellularly trapped fluorescent indicator. *J Cell Biol* 94:325-334.

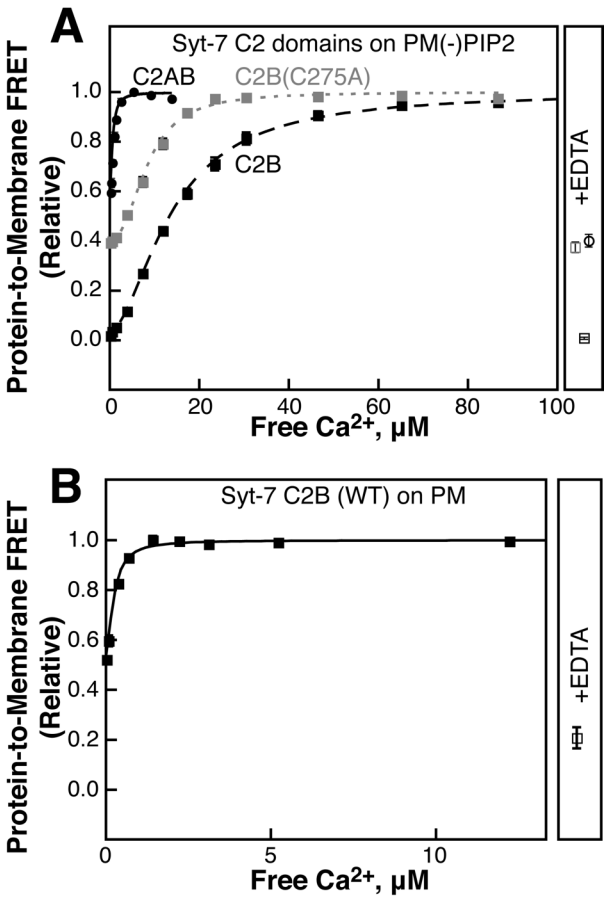

Figure S5: Use of a more aggressive Ca^{2+}-buffering solution to test for Ca^{2+}-independent binding. Ca^{2+} was titrated into solutions containing protein and PM(-)PIP2 (**A**) or PM (**B**) liposomes as described in Methods. The experiments shown here used a Ca^{2+} buffering system containing 1.5 mM NTA, 0.2 mM EDTA, and 1.2 mM total $MgCl_2$ (0.5 mM free $MgCl_2$). The concentrations of free Mg^{2+} and Ca^{2+} were calculated using MaxChelator (https://somapp.ucdmc.ucdavis.edu/pharmacology/bers/maxchelator/webmaxc/webmaxcE.htm). Data were normalized based on best fits to Eq. 1; the parameters from these fits are given in Table 2. Points and error bars shown are mean ± standard deviation of three replicate parallel titrations; where not visible, error bars are smaller than the symbol. Right panels show the extent of reversibility upon addition of 2.5 mM EDTA. Fitting parameters were as follows: C2B (WT) on PM(-)PIP2: initial binding < 5%, $Ca_{1/2}$ 13.9 ± 0.6 µM, H 1.8 ± 0.1; C2B (C275A) on PM(-)PIP2: initial binding 41 ± 1 %, $Ca_{1/2}$ 8.4 ± 0.3 µM, H 2.35 ± 0.08; C2AB on PM(-)PIP2: initial binding 61 ± 1 %, $Ca_{1/2}$ 0.70 ± 0.04 µM, H 1.78 ± 0.03; C2B (WT) on PM: initial binding 53 ± 1 %, $Ca_{1/2}$ 0.24 ± 0.02 µM; H 1.7 ± 0.2. Differences from fitting parameters in Table 2 are within the range of what could be expected based on unavoidable batch variations in liposomes. Importantly, the presence of a Ca^{2+}-independent population persists for each species that had a large membrane-bound fraction prior to Ca^{2+} addition.

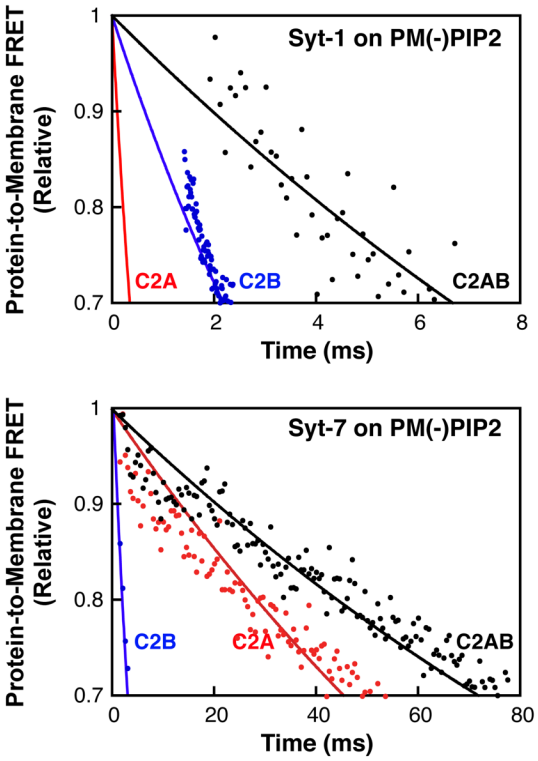

Figure S6: Comparing the rates of initial dissociation kinetics for Syt-1 (top) and Syt-7 (bottom) C2 domains from PM(-)PIP$_2$ liposomes. Shown are magnifications of the first few milliseconds of data from Figures 3B and 4B in the main text, with the y-axes scaled to show only the first 30% of protein dissociation. The C2AB domain of Syt-7 has an initial dissociation rate similar to that of Syt-7 C2A.

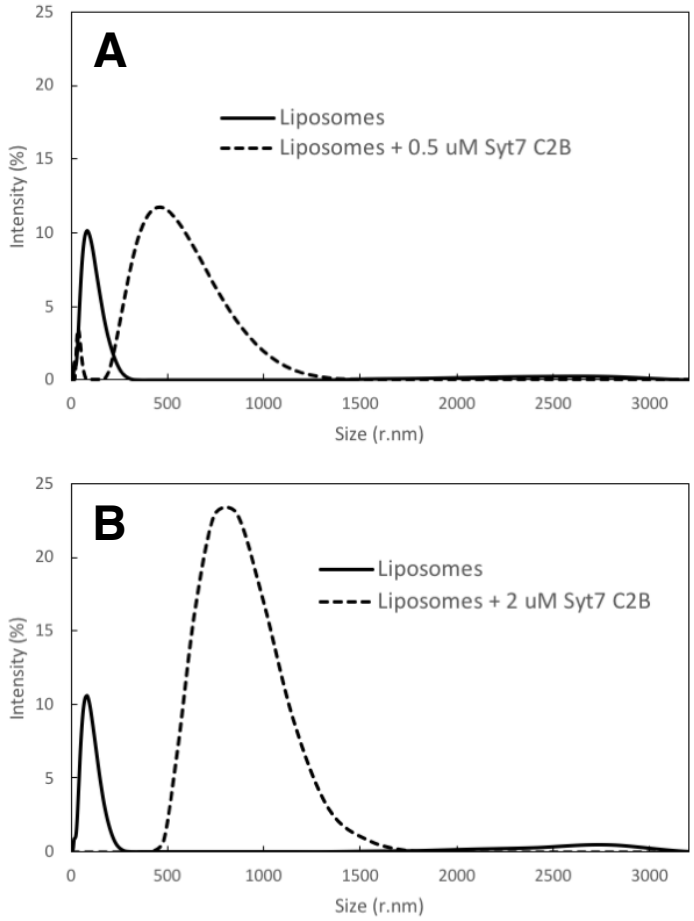

Figure S7. Dynamic light scattering (DLS) of liposome clustering. A total of 0.5 μM **(A)** or 2.0 μM **(B)** Syt-7 C2B (C275A) was added to liposomes (1:1 DOPC/DOPS, 200 μM accessible lipid concentration). Z-averaged intensities are reported. Peaks represent the population of liposomes within certain size range. Data shown are representative of 3 independent replicate measurements.

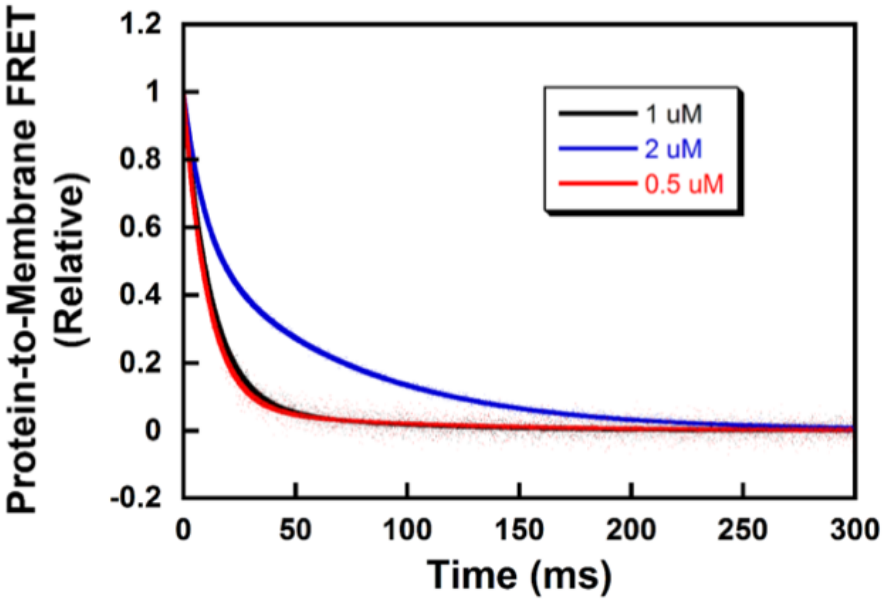

Figure S8. Dissociation kinetics of different concentration of Syt-7 C2B on 1:1 DOPC/DOPS liposomes. Dansyl-PE fluorescence was monitored as solutions containing 0.5 μM (red), 1 μM (black), or 2 μM (blue) protein, 200 μM $CaCl_2$, and liposomes (200 μM accessible lipid) were rapidly mixed with 2 mM EDTA (all concentrations listed are before mixing). Kinetic data were best fit to double exponential decays, with rate constants and respective amplitudes reported in Table S1 below. The signal-to-noise ratio is inversely correlated to the concentration of protein.

Table S1. Dissociation rate constants of Syt-7 C2B from 1:1 DOPC/DOPS are concentration independent while the amplitude of each component of the double exponential fit are well correlated with concentration. Dissociation rate constants were determined from the data shown in Figure S8 as described in Methods. Rate constants and amplitudes from the fast and slow components are shown. Where listed, uncertainties are standard deviations from ≥ 3 separate experiments.

Syt-7 C2B concentration (μM)	**k_{off} (s^{-1})**	
0.5	94 (93% amp)	12 (7% amp)
1	80 ± 9 (88% amp)	13 ± 2 (12% amp)
2	104 (45% amp)	14 (55% amp)

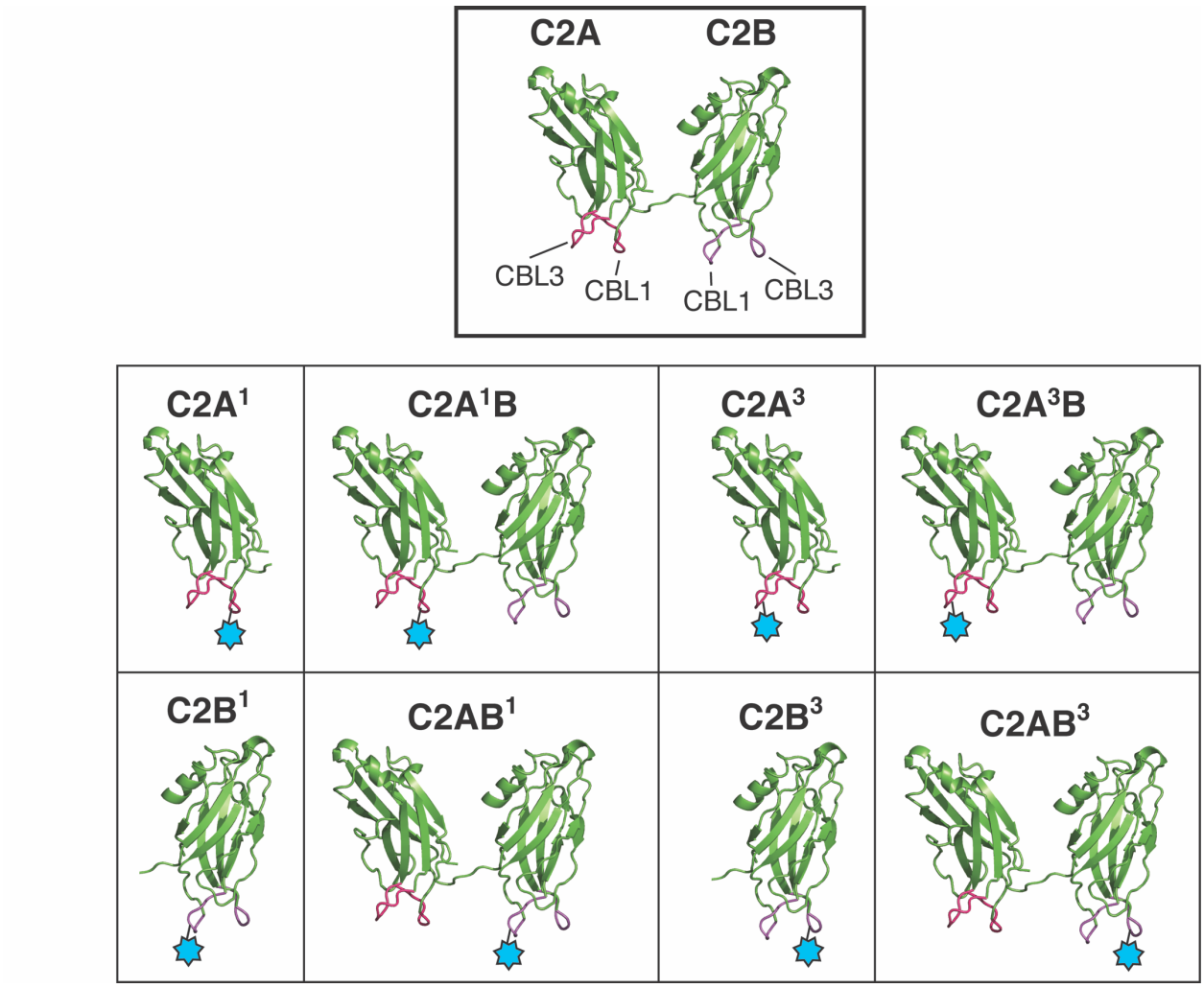

Figure S9: Sites used for AEDANS labeling. *Top:* A composite structural model of Syt-7 C2AB, drawn from structures of the individual domains (PDB IDs: 2D8K for C2A and 3N5A for C2B). Ca^{2+}-binding loops (CBLs) are marked. *Bottom:* Schematic illustrations of AEDANS (cyan stars) labeled protein variants used for membrane insertion experiments.

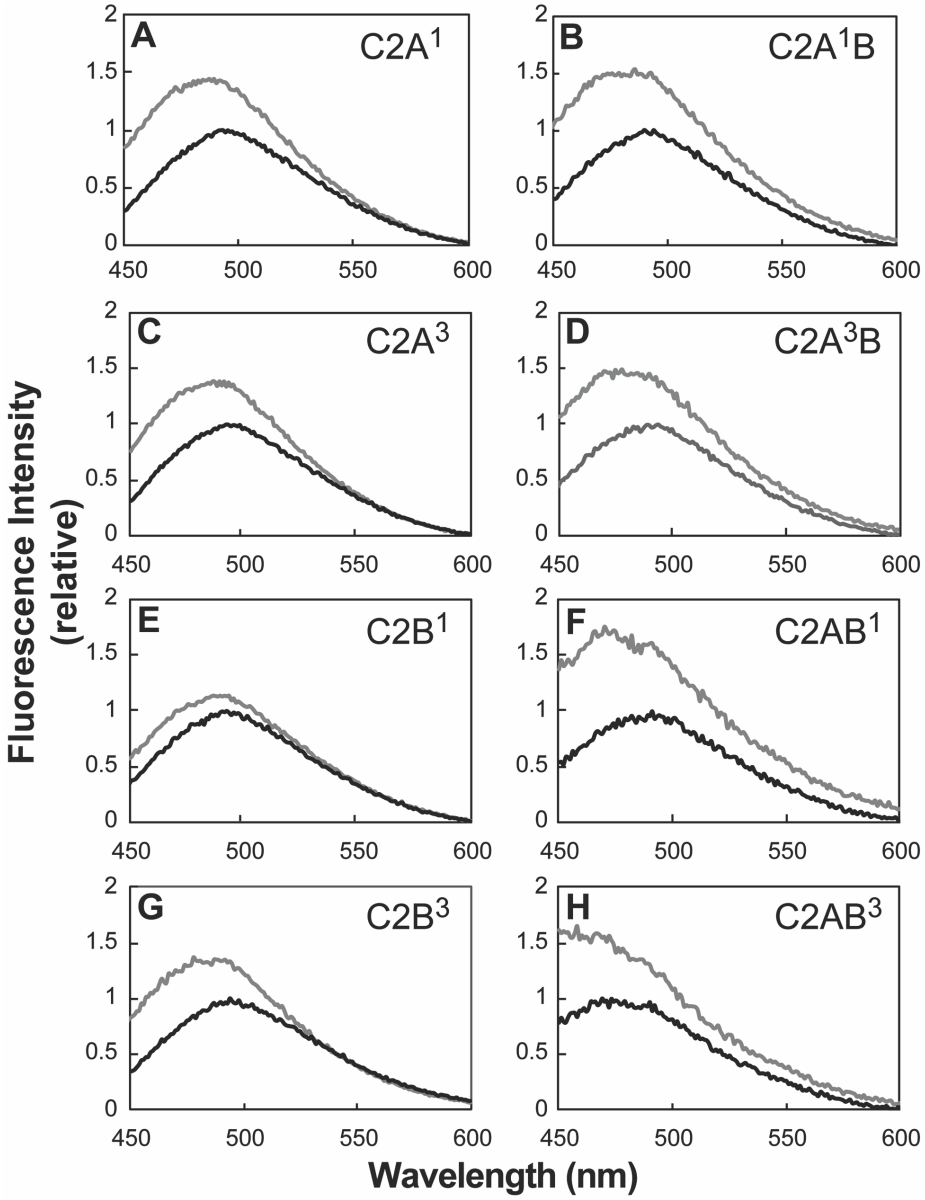

Figure S10. Membrane insertion of Syt-7 C2A and C2B domain loops in the presence of 2% PIP_2. Fluorescence emission spectra are shown of Syt-7 protein domains labeled with AEDANS on the indicated loops (see Figure S9 for schematic and Methods for labeled residues) in solution alone (black) and after addition of PM liposomes (gray). All spectra are normalized to the maximum intensity in the absence of lipid.